Journal of Chemical Research and Innovation
ISSN: 3106-7905 | 3106-7891
Volume 2, Issue 2, 2025

FLUORESCENT SENSING POTENTIAL OF SYNTHESIZED 2′,7′-DICHLOROFLUORESCEIN HYDRAZIDE DERIVATIVES: DESIGN, SYNTHESIS, AND CHARACTERIZATION

Arooj Khan[*1], **Rida Anjum**[2]

[*1,2]*PhD Scholar, Department of Chemistry, University of Faisalabad, Faisalabad, Pakistan*

[*1]aroojkhan78@gmail.com, [2]ridaanjum9012@yahoo.com

Keywords
2′,7′-Dichlorofluorescein, Hydrazides, Aryl Hydrazines, Fluorescent Sensors, Organic Derivatives

Article History
Received: 11 April 2025
Accepted: 21 May 2025
Published: 30 June 2025

Corresponding Author: *
Arooj Khan

Abstract

Optical sensors have become valuable alternatives to traditional sensing systems, offering flexibility for a broad range of analytical applications. Among these, small-molecule fluorescent probes have gained considerable interest due to their ability to detect various environmental and biological analytes, combined with advantages such as simplicity, affordability, and rapid response. Nevertheless, most currently available fluorescent probes are selective for only a single analyte, highlighting the need to design new multifunctional fluorescent compounds. In this study, novel 2′,7′-dichlorofluorescein-based hydrazide derivatives were synthesized using different substituted aryl hydrazines. The reaction progress was monitored through thin-layer chromatography (TLC), while the successful synthesis and structural characterization of the hydrazides were confirmed by Fourier Transform Infrared (FTIR) spectroscopy and proton/carbon nuclear magnetic resonance ($^1H/^{13}C$ NMR) spectroscopy. These newly synthesized hydrazide derivatives exhibit strong potential as multifunctional fluorescent sensing materials for a variety of analytical and environmental applications.

1. INTRODUCTION

One of the significant contemporary problems is the pollution of the environment, and the biosphere's functioning is directly related to the fast global climate change issues we are witnessing at the beginning of the 21st century.[1-8] Pollution of soil, air, and water with heavy metals, organic chemicals, plastic waste, and biological pathogens is dangerous to global health.[9-16]

The most significant environmental issue currently is the contamination of limited waterbodies with tons of toxic waste, including agricultural, sewage, and raw industrial discharge.[12, 17] Addressing these water pollution challenges requires innovative multidisciplinary approaches in environmental pollutant monitoring, detection/sensing, and remediation.[18-20] Water monitoring techniques are extensively employed to identify pollutants across various aquatic ecological applications. In recent decades, research has been undertaken to devise effective and efficient contamination detection strategies with minimal operational costs and energy consumption.[19]

Although some conventional approaches, such as experimental polymerase chain reaction techniques, are often employed for detecting this microbial strain, their use in areas with limited resources is hindered by the substantial cost of equipment and skilled labor.21 Other traditional detection methods, such as chemical sensors and mass spectrometry, have drawbacks, including high complexities, sensitivity to external interferences, and operational expenses. Similarly, while metal detectors, sniffer dogs, and X-ray scanners have demonstrated some success, they still face sensitivity, speed, adaptability, and sensitivity challenges.22

On the other hand, due to their real-time abilities, enhanced sensitivity, and minimum invasiveness, optical sensors have emerged as a viable solution to these limitations and provide an excellent alternative. Consequently, they have grown in popularity and are particularly suitable for uses that involve explosive detection.22 Small-molecule fluorescent probes for detecting ionic and neutral species in biosystems and the environment have gained increasing interest due to their ease of use, affordability, rapid detection capabilities, and outstanding sensitivity and selectivity.23 Until recently, fluorescence probes with various emission signals that respond to numerous analytes have been synthesized. They exhibit remarkable selectivity and sensitivity in aqueous solutions and biological samples, although many were selective for just one analyte.23-27

It is still challenging to synthesize fluorescent probes that exhibit a clear fluorescence response to specific analytes. Consequently, it is vital to develop fluorescent probes that respond to multiple analytes with varying emissions signals. In this context, this research study aims to synthesize and characterize novel 2′,7′-dichlorofluorescein-based hydrazides using different substituted aryl hydrazines. Based on their chemistry, such newly synthesized hydrazides could serve as versatile fluorescent probes for various sensing and detection applications.

1.EXPERIMENTAL

1.1Chemicals

All experiments utilized analytical-grade chemicals without further purification. The 2′,7′- dichlorofluorescein was obtained from Merck. Various substituted phenyl hydrazines and solvents, including methanol, dichloromethane (DCM), and ethanol, were purchased from Sigma-Aldrich.

3.2. Synthesis Procedure

Ethanol was added as a solvent to the round-bottom flask. The stoichiometric amounts of 2′,7′- dichlorofluorescein (1 mmol), and respective aryl hydrazine (1.25 mmol) were included. The entire system was carefully subjected to reflux. It was regularly examined every 30 minutes. After approximately 12 hours, some color changes were observed in the system. The chemical changes in the reaction mixture were periodically assessed using TLC. The solid product was combined with ethyl acetate, washed with water, and separated by filtration. TLC was performed to determine the purity of the product. The mobile phase for TLC consisted of 9 ml of chloroform and 1 ml of methanol. The ratio of chloroform to methanol was adjusted to modify the polarity of the mixture. The general reaction equation is given in Scheme 1.

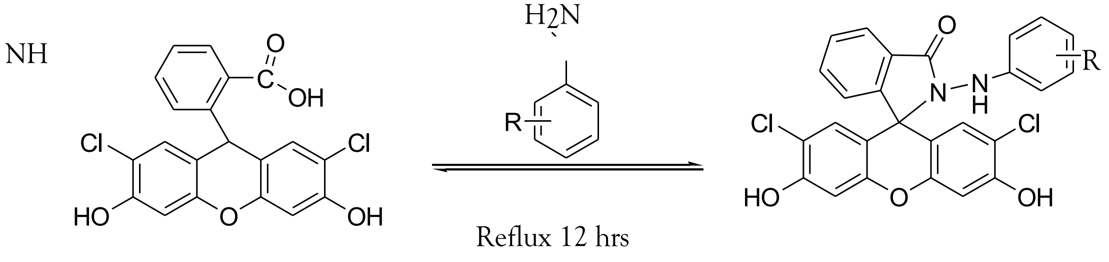

Where R= Cl, F, Br, CN & Iso-propyl

Scheme 1. The general reaction of 2′,7′-dichlorofluorescein with different aryl hydrazine.

2.3. Characterization

TLC was performed at 30-minute intervals to monitor the reaction's progress and confirm product formation. TLC plates with silica coating were utilized, and spots were visualized under ultraviolet light at 254 and 366 nm wavelengths. The mobile phase for TLC consisted of DCM and methanol in a 9:1 ratio. Agilent 630 series spectrometer was used to obtain FTIR spectra. Bruker Avance DPX FT-NMR spectrometer was employed to acquire ^{1}H (500 MHz) and ^{13}C (125 MHz) NMR spectra (δ in ppm).

2. RESULTS AND DISCUSSION

2.1. 2′,7′-dichloro-2-((2-chlorophenyl) amino)-3,6-dihydroxyspiro [isoindoline-1-9-xanthen]- 3-one:

Fade yellow color, 71% yield, DMSO solubility. IR (KBr) cm^{-1} 3051, 3000, 1585.49, 750, 850; ^{1}HNMR (500 MHz, DMSO-*d6*) δ10.86 (s, 1H), 8.11 (s, 2H), 7.93 (d, 1H),7.92 (d, 2H), 7.76 (t, 1H), 7.74 (t, 1H), 7.73 (t, 3H), 7.70 (t, 1H), 6.3 (s, 1H), 6.57 (d, 3H); ^{13}CNMR (125 MHz, DMSO-*d6*) 64.84, 104.11, 110.12, 110.96, 114.76, 116.07, 123.70, 124.76, 128.88, 130.13, 130.37, 131.25, 134.53, 147.29, 149.00, 151.77, 154.61, 165.32

2.2. 2′,7′-dichloro-2-((3-bromophenyl) amino)-3,6-dihydroxyspiro[isoindoline-1-9-xanthen]- 3-one:

Fade yellow color, 70% yield, DMSO solubility. IR (KBr) cm^{-1} 3381, 1591, 1099, 815; ^{1}HNMR (500 MHz, DMSO*d6*) 10.88 (s, 1H), 8.18 (s, 1H), 7.95 (d, 1H), 7.77(t, 1H), 7.57(t, 1H), 7.32 (d, 1H,), 6.94 (t, 1H,) 6.56 (s, 2H); ^{13}CNMR (125 MHz, DMSO-*d6*) δ 60.23, 104.14, 110.96, 111.94, 114.80, 116.23, 121.75, 122.16, 123.75, 124.82, 128.77, 130.22, 130.34, 130.62, 134.63, 148.80, 149.72, 151.83, 154.71, 165.37, 170.83.

2.3. 2′,7′-dichloro-2-((4-isopropylphenyl) amino)-3,6-dihydroxyspiro[isoindoline-1-9-xanthen]-3-one:

Fade yellow color, 66% yield, DMSO solubility. IR (KBr) cm^{-1} 3282, 1581, 1101, 719; ^{1}HNMR (500 MHz, DMSO-*d6*) δ 10.84 (s, 1H), 8.02 (d, 1H), 7.91 (t, 3H,); 7.34 (s, 1H), 6.93 (s, 1H), 6.80 (m, 4H), 6.55 (s, 1H), 6.34 (d, 2H), 2.69 (pentet, 1H), 1.22 (d, 6H);^{13}CNMR (125 MHz, DMSO-*d6*) δ 24.54, 32.93, 64.87, 104.10, 111.19, 113.09, 115.97, 123.51, 124.73, 126.41, 128.98, 130.07, 130.50, 134.40, 139.42, 146.00, 149.34, 151.75, 154.51, 165.63.

2.4. 2′,7′-dichloro-2-((4-fluorophenyl) amino)-3,6-dihydroxyspiro[isoindoline-1-9-xanthen]- 3-one:

Fade orange color, 75% yield, DMSO solubility. IR (KBr) cm^{-1} 3444, 1514, 1118, 719; ^{1}HNMR (500 MHz, DMSO-*d6*) δ 10.83 (s, 1H), 7.96 (d, 1H), 7.78(t, 1H), 7.75(d, 1H), 7.71 (s, 1H), 7.32 (d, 1H) 7.21(d, 1H), 6.96 (t, 1H), 6.77 (s, 1H), 6.61 (s, 1H), 6.54 (s, 1H) 6.40 (d, 1H); ^{13}CNMR (125 MHz, DMSO-*d6*); δ 65.12, 103.90, 110.83, 114.25, 115.88, 117.92, 120.66, 123.69, 124.83, 127.27, 129.37, 129.51, 130.18, 130.50, 134.56, 143.28, 148.82, 151.96, 154.55, 165.18

2.5. 2′,7′-dichloro-2-((4-cyanophenyl)amino)-3,6-dihydroxyspiro[isoindoline-1-9- xanthen]-3-one:

Fade orange color, 74% yield, DMSO solubility. IR (KBr) cm^{-1} 3392, 2140, 1558, 1099; ^{1}HNMR (500 MHz, DMSO-*d6*) δ 10.83 (s, 1H), 8.20 (s, 1H), 7.95(s, 1H), 7.71 (t, 1H), 7.28 (d, 2H), 7.14 (d, 2H), 6.93(t, 1H), 6.58 (s, 2H), 6.41 (d, 2H);^{13}CNMR (125 MHz, DMSO-*d6*) δ 48.57, 64.37, 103.61, 110.45, 111.05, 111.44, 115.68, 118.32, 123.25, 124.32, 128.33, 129.69, 129.81, 129.85, 133.14, 134.11, 148.35, 149.12, 151.30, 154.19, 164.85.

Although FTIR, ^{1}H NMR, and ^{13}C NMR spectra of all compounds were obtained. Here, we delve further into chloro **(Figure 1A)** and cyano **(Figure 1B)** derivatives. FTIR spectra were used to identify functional groups in compounds. In the case of chloro, peaks at 1585.49 and 3051 cm^{-1} are characteristic of amide C=O and N-H stretches, respectively. A broad peak at around 3000 cm^{-1} refers to aromatic rings, whereas two peaks between 750 and 850 cm^{-1} correspond to two types of chloride groups. Similarly, an intense peak for the cyano derivative at 1558 cm^{-1} corroborates the amide C=O stretching. Furthermore, the characteristic peaks of C-N, C-H, and N-H stretching vibrations at 1099, 2914, and 3392 cm^{-1} confirm the formation of the cyano derivative. The ^{1}HNMR analysis was performed for the structural elucidation of the chloro derivative in DMSO at 500 MHz frequency. The aromatic ring's protons were observed in the 7.93 to 6.57 ppm range, whereas the N-H proton was a singlet at 6.3 ppm. The protons (5 and 10 positions) with a *J* value of 7.5 Hz were identified as a doublet at 7.92 ppm, whereas protons at positions 2 and 3 appeared as a multiplet. A triplet of protons (2' and 3') appeared at 7.76 ppm with coupling constants of 7.5 and 7 Hz for ortho and meta coupling, respectively. A doublet of a doublet at 6.57 Hz could be assigned to a proton at 4 position with a *J* value of 2 Hz. The presence of protons at the 7 and 8 positions as a singlet may be attributed to the symmetry of the fluorophore.

The ^{13}C-NMR spectrum of the chloro derivative provides crucial information regarding its molecular structure. The signal at 64.84 ppm corresponds to the spiro carbon, a characteristic feature of the xanthenone core. The chemical shifts ranging from 104.11 to 165.32 ppm indicate the presence of aromatic carbons within the isoindoline-xanthenone framework. The 104.11 and 110.12 ppm peaks suggest carbons adjacent to oxygen, likely attributed to the hydroxyl-substituted positions. The signals observed at 110.96, 114.76, and 116.07 ppm correspond to additional aromatic carbons, possibly influenced by the electron-withdrawing chlorine atoms. The peaks at 123.70, 124.76, 128.88, 130.13, 130.37, and 131.25 ppm represent benzene ring carbons, including those attached to chlorine atoms, causing slight deshielding. The downfield signals at 147.29, 149.00, and 151.77 ppm indicate carbons bonded to electronegative oxygen or nitrogen, supporting the presence of hydroxyl and amino groups. The peak at 154.61 ppm likely corresponds to a carbonyl or conjugated system within the xanthenone structure. In contrast, the signal at

165.32 ppm is attributed to the most deshielded carbon, likely the carbonyl carbon of the spiro-lactone system. These NMR chemical shifts confirm the structural integrity of the molecule, thereby supporting its functionalized aromatic nature.

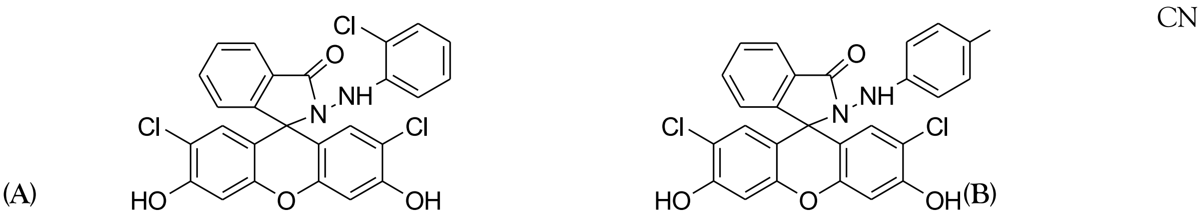

Figure 1. Structures of (A) chloro and (B) cyano derivatives of 2′,7′-Dichlorofluorescein.

3. CONCLUSION

Fluorescent organic derivatives have been excellent probes for sensing various substances in different media and systems. Despite their simplicity, affordability, and efficient detection potential, such probes' distinct fluorescence response to particular analytes remains challenging. In the present research, we synthesized new 2′,7′-dichlorofluorescein-based hydrazides using different substituted aryl hydrazines. Subsequently, these fluorescent organic derivatives were characterized using analytical tools, including FTIR and NMR techniques. The chemical properties of these fluorescent hydrazides indicate their potential to address existing challenges and show promising prospects in various practical applications, such as biosensing and environmental monitoring.

REFERENCES

Mudassir, M. A.; Aslam, H. Z.; Ansari, T. M.; Zhang, H.; Hussain, I. Fundamentals and Design-Led Synthesis of Emulsion-Templated Porous Materials for Environmental Applications. *Advanced Science* **2021**, *8* (22), 2102540.

Mudassir, M. A.; Kousar, S.; Ehsan, M.; Usama, M.; Sattar, U.; Aleem, M.; Naheed, I.; Saeed, O. B.; Ahmad, M.; Akbar, H. F. Emulsion-Derived Porous Carbon-Based Materials for Energy and Environmental Applications. *Renewable and Sustainable Energy Reviews* **2023**, *185*, 113594.

Malhi, Y.; Franklin, J.; Seddon, N.; Solan, M.; Turner, M. G.; Field, C. B.; Knowlton, N. Climate Change and Ecosystems: Threats, Opportunities and Solutions. The Royal Society: **2020**; Vol. 375, p 20190104.

Mudassir, M. A.; Tazeen, Z.; Kousar, S.; Li, M.; Zhao, X. Metal–Organic Framework/Graphene-Based Nanocatalysts for Hydrogen Evolution Reaction: A Comprehensive Review. *International Journal of Hydrogen Energy* **2025**, *98*, 1299-1313.

Mudassir, M. A.; Batool, M.; Kousar, S.; Makarem, M. A.; Razia, E. T.; Meshksar, M.; Murtaza, M.; Tariq, K.; Din, M. A. U.; Bodlah, M. A. Plasma-Assisted Hydrodeoxygenation of Bio-Oils. *Fuel Processing Technology* **2023**, *250*, 107872.

Maria Batool, M. A. M., Shazia Kousar, Mohammad Amin Makarem,. Carbon Capture by Hybrid Separation. In *Encyclopedia of Renewable Energy, Sustainability and the Environment*, First ed.; Rahimpour, M. R. Ed.; Vol. 4; Elsevier, **2024**; pp 935-942.

Gul, H.; Sadia Nasrullah, S.; Mudassir, M. A.; Kousar, S.; Mazari, M. E.; Bodlah, M. A.; Makarem, M.

Carbon Capture by Amine- and Liquid-Modified Adsorbents. In *Encyclopedia of Renewable Energy, Sustainability and the Environment*, First ed.; Rahimpour, M. R. Ed.; Vol. 4; Elsevier, **2024**; pp 671-680.

Mudassir, M. A.; Saleem, S.; Kousar, S.; Rafiq, A.; Ahmad, I.; Makarem, M. A. Carbon Capture and Utilization by MXene-Based Materials. In *Encyclopedia of Renewable Energy, Sustainability and the Environment*, First ed.; Rahimpour, M. R. Ed.; Vol. 4; Elsevier, **2024**; pp 943-964.

Münzel, T.; Hahad, O.; Daiber, A.; Landrigan, P. J. Soil and Water Pollution and Human Health: What Should Cardiologists Worry About? *Cardiovascular research* **2023**, *119* (2), 440-449.

Mudassir, M. A.; Ullah, Z.; Kousar, S.; Majeed, H.; Nazir, F.; Ali, B.; Makarem, M. A. Artificial Intelligence for Developing Smart and Sustainable Energy Systems. In *Encyclopedia of Renewable Energy, Sustainability and the Environment*, First ed.; Rahimpour, M. R. Ed.; Vol. 4; Elsevier, **2024**; pp 943-964.

Arif, S.; Mudassir, M. A.; Kousar, S.; Rahim, U.; Makarem, M. A.; Kiani, P. Upgrading Bioenergy Materials to Chemicals. In *Encyclopedia of Renewable Energy, Sustainability and the Environment*, First ed.; Rahimpour, M. R. Ed.; Vol. 1; 2024; pp 849-860.

Mudassir, M. A.; Hussain, S. Z.; Rehman, A.; Zaheer, W.; Asma, S. T.; Jilani, A.; Aslam, M.; Zhang, H.; Ansari, T. M.; Hussain, I. Development of Silver-Nanoparticle-Decorated Emulsion-Templated Hierarchically Porous Poly(1-Vinylimidazole) Beads for Water Treatment. *ACS applied materials & interfaces* **2017**, *9* (28), 24190-24197.

Mudassir, M. A.; Hussain, S. Z.; Kousar, S.; Zhang, H.; Ansari, T. M.; Hussain, I. Hyperbranched Polyethylenimine-Tethered Multiple Emulsion-Templated Hierarchically Macroporous Poly(Acrylic Acid)–Al2O3 Nanocomposite Beads for Water Purification. *ACS Applied Materials & Interfaces* **2021**, *13* (23), 27400-27410.

Mudassir, M. A.; Hussain, S. Z.; Khan, M.; Asma, S. T.; Iqbal, Z.; Huma, Z.; Ullah, N.; Zhang, H.; Ansari, T. M.; Hussain, I. Polyacrylamide Exotemplate-Assisted Synthesis of Hierarchically Porous Nanostructured Tio2 Macrobeads for Efficient Photodegradation of Organic Dyes and Microbes. *RSC advances* **2018**, *8* (52), 29628-29636.

Akhter, N.; Batool, M.; Yaqoob, A.; Shahid, M.; Muhammad, F.; Khan, J.; Mudassir, M. A.; Rasheed, M.; Javed, S.; Al Farraj, D. A. Potential Biological Application of Silver Nanoparticles Synthesized from *Citrus paradisi* Leaves. *Scientific Reports* **2024**, *14* (1), 29028.

Batool, M.; Qazi, R.-e.-M.; Mudassir, M. A.; Sajid, Z.; Zaman, R.; Rauf, M. A.; Kousar, S.; Ahmad, I.; Rehman, F. U.; Mian, A. A. Titania–Graphene Oxide Nanocomposite-Based Philadelphia-Positive Leukemia Therapy. *ACS Applied Bio Materials* **2024**, 7, 4352-4365.

Mudassir, M. A.; Hussain, S. Z.; Jilani, A.; Zhang, H.; Ansari, T. M.; Hussain, I. Magnetic Hierarchically Macroporous Emulsion-Templated Poly(Acrylic Acid)–Iron Oxide Nanocomposite Beads for Water Remediation. *Langmuir* **2019**, *35* (27), 8996-9003.

Liu, X.; Sathishkumar, K.; Zhang, H.; Saxena, K. K.; Zhang, F.; Naraginiti, S.; Anbarasu, K.; Rajendiran, R.; Aruliah, R.; Guo, X. Frontiers in Environmental Cleanup: Recent Advances in Remediation of Emerging Pollutants from Soil and Water. *Journal of Hazardous Materials Advances* **2024**, 100461.